Solution Casted Cellulose Acetate films. Influence of Surface Substrate and Humidity on Wettability, Morphology and Optical Properties

Ana Kramar (akramar@ing.uc3m.es)
Universidad Carlos III de Madrid Departamento de Ciencia e Ingenieria de Materiales e Ingenieria Quimica

Irene Rodríguez Ortega
Universidad Carlos III de Madrid

Gustavo González-Gaitano
Universidad Pública de Navarra: Universidad Publica de Navarra

Javier González-Benito
Universidad Carlos III de Madrid Departamento de Ciencia e Ingenieria de Materiales e Ingenieria Quimica

Research Article

Keywords: cellulose acetate, films, solution casting, morphology, crystallinity, micropatterning

Posted Date: March 24th, 2022

DOI: https://doi.org/10.21203/rs.3.rs-1389706/v1

Abstract

Variations on the processing conditions of conventional methods for polymeric film preparation may allow tuning certain properties of film. Different casting surfaces and humidity during casting are presented in this work, as variables to be considered for cellulose acetate film preparation (CA). Casting surfaces, borosilicate glass, soda-lime glass and Teflon (PTFE) dish are used and their influence on various properties of CA films is assessed. Soda-lime glass was coated with chlorotrimethylsilane because CA is strongly adhered to the neat surface during drying, making the film detachment impossible. The surfaces of glass dishes are smooth, while PTFE surface has a distinctive pattern, which is adopted by casted films upon drying. The resulting patterned morphology of the films is studied using optical profilometry. Patterned films are translucent while smooth surface films are transparent. Apart from the effect of different surface types, humidity influence on CA films is evaluated in terms of conditions during the evaporation of solvent from solution (35 %, 55 % and 75 % humidity). The increase of the humidity produces smoother surfaces and higher film crystallinity compared to films casted in open air; however, wettability of films does not seem to be influenced by this variable, except for a higher hydrophobicity in the patterned films. Due to the specific morphology of the patterned films, change in opacity upon wetting is detected, going from translucent to transparent, while removal of water from the surface restores the translucency. This approach can be used for preparation of patterned films for food packaging application which can serve as humidity sensor.

1. Introduction

Cellulose acetate is one of the most important derivatives of cellulose that is recently coming into focus of research interest for the production of nanofibers and films for food packaging (Espitia et al. 2011; Paunonen 2013; Vartiainen et al. 2014; Do Socorro Rocha Bastos et al. 2016; El Fawal et al. 2019). Cellulose acetate has excellent film forming capabilities; it is chemically and thermally stable and, most importantly, biodegradable, biocompatible and non-toxic. Its current use is mostly in textile fibers, filters and eyewear frames (Kamide 2005; Menachem 2007). Research into the possible use of cellulose acetate films aims, besides at food packaging (Espitia et al. 2011; Vartiainen et al. 2014; Do Socorro Rocha Bastos et al. 2016; El Fawal et al. 2019), at adsorption of pollutants from water (De Carvalho Eufrásio Pinto et al. 2019; Gopi et al. 2019), water filtration in general (Filho et al. 2004; Vinodhini et al. 2017), filtration of water polluted with microorganisms (Xie and Hung 2019), and preparation of conductive polymer based films by addition of copper (Shivamurthy et al. 2019).

Cellulose acetate is easily soluble in acetone. The preparation of films using solution casting method of acetate solution in this solvent is a very robust and simple method (Wu et al. 2014; Gonçalves et al. 2019), investigations being mainly focused on preparation of cellulose acetate films from its solution, either standalone or mixed with other polymers (Yang et al. 2013). The usual procedure for polymer casting consists of preparing and pouring the solution on a mold or substrate, and then leave the system until the solvent evaporates under controlled conditions (Yang et al. 2013; Do Socorro Rocha Bastos et al. 2016; El Fawal et al. 2019; Rodríguez et al. 2019; Yadollahi et al. 2019; Lyytikäinen et al. 2021). However,

there are very few investigations about the influence of environmental parameters during casting such as humidity or type of casting surface on the resulting properties of films as, for instance, wettability and optical behavior.

Recently, Lyytikainen et al. (2021) have studied the effect of drying temperature when casting on the wetting and barrier properties of films prepared from various cellulose derivatives, methyl cellulose, hydroxyethyl cellulose and microfibrilated cellulose. They concluded that the surface roughness of glass petri dishes used as substrate surface for casting can induce formation of air bubbles trapped in the films obtained by drying at higher temperatures (50°C), affecting the morphology and consequently the barrier properties of the films.

On the other hand, an interesting investigation explored different optical properties of cellulose based films by casting microfibrilated pulp on hydrophilic and hydrophobic surfaces (Mirvakili et al. 2021). Opaque or translucent films were produced by self-assembly of microfibrilated cellulose pulps on different casting surfaces. The hydrophobic surface of PTFE induced the assembly of microfibers in such way that it yielded convex, translucent films, while a hydrophilic glass surface led to a concave self-assembly, producing opaque microfibrilated cellulose films.

Harini and Sukumar (2019) compared open air drying and vacuum drying for preparation of cellulose acetate films on Petri dishes and found that transparent films were obtained in vacuum drying, while white films formed by open air drying. Authors claimed that open air drying induced increased order in CA films, causing higher crystallinity and consequently whitish appearance (Harini and Sukumar 2019). However, they did not comment on the effects of the material the Petri dishes were made of, on the material properties.

Considering the above mentioned, there is not yet a clear answer about the origin of the specific optical properties and visual appearance of films induced by the environmental conditions, as well as the subjacent mechanisms depending on the choice of particular casting conditions. It is clear that this information could help in the future to tune the properties in terms of visual appearance of CA films in a very simple way, which is the motivation of the present work

In this investigation, the influence of the room relative humidity and the substrate support on cellulose acetate, CA, casted films is studied. Different concentrations of CA in acetone are used as casting solutions under different humidity levels, which are compared with the ones casted in an open air without humidity control. Moreover, the influence of casting substrate surfaces (borosilicate glass, soda-lime glass and micropatterned Teflon-PTFE) on the morphological, structural, thermal, and wetting properties is also studied.

2. Materials And Methods

2.1. Experimental Material

Cellulose acetate, CA (Sigma Aldrich, average Mn ~ 30000) was used for preparation of casted films. Acetone (Sigma Aldrich, HPLC Plus ≥ 99.9% purity) as solvent and chlorotrimethylsilane (Alfa Aesar 98+%) as coating agent for soda-lime glass, were used as received without further purification. Salt solutions of $MgCl_2$ (Sigma Aldrich, 98% purity), $Mg(NO_3)_2 \cdot 6H_2O$ (Labkem, 99.5% purity) and $CH_3COONa \cdot 3H_2O$ (Sigma Aldrich, 99% purity) were prepared using distilled water.

2.2. Casting of films

Solutions of cellulose acetate, CA, 8%, 10% and 12% (w/v) were prepared by dissolving the polymer in powder form in the required amount of acetone. Each casted sample was prepared by depositing 0.1 $ml \cdot cm^{-2}$ of solution onto a casting dish. A set of solutions at the three concentrations was casted first at open air (temperature 22 ± 2 ºC and 35 ± 5% humidity) on different circular dishes made of borosilicate glass, soda-lime glass and PTFE. On the other hand, the same set of solutions was also casted placing the casting dishes in a perforated box (Fig. 1), fixing the humidity at least 24 hours prior to casting to ensure its stabilization. Relative humidity inside the box was controlled with a saturated saline solution ($MgCl_2$ for 35% of humidity; $Mg(NO_3)_2 \cdot 6H_2O$ for 55% ; and $CH_3COONa \cdot 3H_2O$ for 75%). The temperature during casting was 22 ± 2 ºC.

The holes made in the box help to remove the solvent from the casting chamber and keep the desired humidity. Films were the left to dry 24 hours until complete evaporation of the solvent, and then detached from the surface and stored in aluminum foil for further analysis.

2.3. Characterization methods

The morphology of samples was investigated using an optical profilometer Olympus DSX500 (Olympus Iberia, Barcelona, Spain). Roughness parameters were obtained according to the standard EN ISO 4288 (1997), specifically *Ra* (arithmetic mean roughness) and *Sa* (surface arithmetic mean height) over a sample area of 1499·1499 μm. In the case of *Ra*, an average was taken from six linear profiles (3 in the X direction and 3 in the Y direction). Samples were observed on the upper (in contact with air during drying) and down (in contact with the casting surface) sides, respectively. The cut-off wavelength λc to carry out the fittings in the roughness analysis was chosen according to standard EN ISO 4288.

Wettability was evaluated by measuring the contact angle between distilled water and CA films using an OCA-15 Plus Goniometer (Data Physics, Neurtek Instruments, Eibar, Spain) and following the sessile drop method. The contact angles were the average of 4 measurements per each side of the specimens. In order to evaluate the evolution of wetting, photographs of the water drops (3 μl volume) on the surfaces of the materials were taken as a function of time up to 300 s, measuring at each time the corresponding contact angles.

Thermal behavior and crystallinity were studied by differential scanning calorimetry, DSC, using a Mettler Toledo 822e calorimeter, under nitrogen atmosphere. Approx. 4.5-5 mg of sample was tested according to the following thermal cycles: a) from 50 to 300 ºC at a heating rate of 10 ºC/min; b) isothermal step at 300 ºC for 5 min; c) from 300ºC to 50ºC at a cooling rate of 10 ºC/min, and d) a second heating cycle

from 50 to 300 ºC at 10ºC/min. The crystalline fraction of the casted materials, χ, was calculated from the first heating cycle by dividing the enthalpy of fusion of the samples by that of a 100% crystalline triacetate cellulose, 58.8 $J \cdot g^{-1}$ (Cerqueira et al. 2006).

Attenuated total reflectance Fourier transformed infrared spectroscopy, ATR-FTIR, spectra were recorded on a Shimadzu IRAffinity-1S spectrometer equipped with a Golden Gate ATR accessory (diamond window), from 600 to 4000 cm^{-1} with a resolution of 4 cm^{-1} and averaging 32 scans. Each sample was measured two times at different locations on both sides of the films. Spectra were analyzed using the KnowItAll Spectroscopy software (Academic edition, Willey Science Solutions).

3. Results And Discussion

3.1. Influence of casting conditions on morphology of films

Films casted on glass at open air, compared to the ones casted under controlled humidity, show much higher unevenness and defects (Fig. 2). This is probably due to non-controlled air flow over the films when drying at open air, leading to a faster evaporation rate at humidity lower than 35%. As can be seen in Fig. 2, the films obtained at open air (OA) were not smooth, showing a wrinkled and bumpy surface. However, films casted under controlled humidity show a much smoother appearance, although with slightly lower transparency the higher the humidity is.

When films are observed with the optical profilometer, interesting features can be noticed (Fig. 3). The films casted at open air and 35% humidity exhibited throughout the sample a hexagonal-like pattern generated by accumulation of material at the hexagon edges, probably due to a surface tension effect induced by the fast evaporation rate that occurs when the relative humidity is low enough and air currents are present. However, under controlled humidity casting, the rate of solvent evaporation is slower. At low humidity (35%), some defects, similar to those present when casting films at open air (at the same humidity) could be seen but, in general, films appear more uniform and flat. Increasing the humidity up to 55% led to the disappearance of these patterns on the upper side of the films. It seems therefore that these particular morphological features observed on OA films are a consequence of the low humidity environment and fast evaporation. Under higher humidity conditions, even though the temperature remains constant, the solvent evaporates more slowly due to saturated humid air above the surface. In films casted at 75% of humidity, occasionally defects in the form of trapped air bubbles can be seen (Fig. 3). However in these films, flatness is preserved and no large defects were found, but casted films became whitish (as can be seen in Fig. 2). A possible explanation to this is an increase in the crystallinity, since crystalline domains may scatter light (Harini and Sukumar 2019). Crystallinity was further studied and presented in the next section.

At open air evaporation conditions, the same hexagonal pattern was observed on upper side of the films regardless the surface of casting (glass and PTFE). In other words, when PTFE is used, the hexagonal-like pattern could be also observed on the upper side of the casted film in contact with air during solvent

evaporation, which suggests that the upper side film topography is not induced by the morphology of the PTFE surface. In fact, the surface of the film directly in contact with the PTFE, showed in all cases a very different pattern, in the form of circular channels, as it can be seen in Fig. 4.

The films casted on PTFE at 55% of humidity had a pattern on the down side but they were flat on the side directly in contact with air, not showing the hexagonal features as in the ones casted at open air. Furthermore, regardless of humidity, their overall appearance was translucent (Fig. 4f). The pattern induced by the topography of the PTFE surface may be the cause of the light scattering leading to the translucent appearance. Measurement of the dimensions of the circular channels observed in the films casted from PTFE lead to a width of 40.6 μm ± 1.5 μm and depth of 1.2 ± 0.4 μm (average of 10 measurements). Since the depth of these channels is up to approx. 1 μm and they have concave shape, their geometry is comparable to a wavelength of visible light which could be the reason for scattering of light and opacity.

Roughness of the films (Table 1) was found to be independent on the polymer concentration of the solutions, without significant differences between the upper and down sides. There is only a slightly difference between the samples casted from 8% and 10% CA, at 35% humidity, when compared to the surfaces in direct contact with the dish (down side) and those in contact with the air (upper side). Furthermore, the standard deviations for the roughness parameters were higher for the films prepared at 35% of humidity and decreased when increasing the humidity, suggesting that the film heterogeneity increases, despite the similar roughness.

Table 1
Influence of humidity, solution concentration and casting surface type on roughness parameters.

Concentration of solution	humidity	side of film	*Ra*, µm	*Sa*, µm
8%	coated glass 35%	upper side	7.7 ± 2.2	10.0
		down side	10.4 ± 2.5	13.6
	coated glass 55%	upper side	8.1 ± 1.5	8.4
		down side	7.6 ± 1.4	9.0
	coated glass 75%	upper side	8.3 ± 1.5	9.2
		down side	6.6 ± 1.1	8.5
	PTFE at 55%	upper side	4.2 ± 1.0	4.9
		down side	2.4 ± 0.25	2.6
10%	coated glass 35%	upper side	9.2 ± 2.6	10.7
		down side	12.4 ± 2.8	13.8
	coated glass 55%	upper side	7.4 ± 1.5	8.4
		down side	8.4 ± 3.1	12.0
	coated glass 75%	upper side	7.8 ± 1.7	8.5
		down side	7.4 ± 0.9	9.2
	PTFE at 55%	upper side	4.0 ± 0.6	4.7
		down side	5.3 ± 1.1	6.8
12%	coated glass 35%	upper side	8.6 ± 2.0	10.7
		down side	7.1 ± 1.6	10.1
	coated glass 55%	upper side	7.1 ± 1.5	10.4
		down side	8.0 ± 0.7	15.7
	coated glass 75%	upper side	8.8 ± 2.0	10.8
		down side	7.9 ± 2.4	10.1
	PTFE at 55%	upper side	3.1 ± 0.4	3.5
		down side	3.4 ± 0.6	4.6

There is not a clear trend of the roughness as a function of humidity, but important differences can be observed depending on the dish type. Thus, regardless the concentration and for a relative humidity of

55%, when PTFE is used for solvent casting, CA films presented 48% less roughness in both upper and down sides compared with glass casted films (Table 1). The difference in roughness can be due to variations in the evaporation rate depending on the nature of the substrate used for solvent casting. When a glass dish is used, polymer films are more easily detached from surface compared to the ones casted on PTFE dish.

3.2. Influence of casting conditions on structural properties of films

A potential structural variation on the films depending on the casting conditions was studied by ATR-FTIR spectroscopy. The films obtained from polymer solutions of 10% concentration were considered as representative ones (Fig. 5).

In each case, typical absorption bands of cellulose acetate were observed. The broad band around 3400 cm^{-1} is assigned to non-esterified hydroxyl groups of cellulose, while the weak band at 2945 cm^{-1} is associated to the CH antisymmetric stretching of the CH_3, which is slightly shifted to 2949 cm^{-1} in the case of film casted at 75% humidity, along with the weak band at 2886 cm^{-1} associated to CH_3 symmetric stretching. There strong absorption at 1737 cm^{-1} corresponds to the carbonyl group stretching, as expected for cellulose acetate, which does not change under the processing conditions used to prepare the films. The peak at 1369 cm^{-1} corresponds to the symmetric CH_3 bending band is also distinguished, along with the antisymmetric and symmetric bands for the C-O-C stretching of the ester groups, at 1219 cm^{-1} and 1033 cm^{-1}, respectively (Gonçalves et al. 2019; Figueiredo et al. 2020). Finally, the characteristic peak at 904 cm^{-1} is assigned to acetate methyl groups (Figueiredo et al. 2020). After a thorough analysis of the spectra, it can be concluded that the nature of the substrate to carry out the casting and the humidity conditions did not affect the molecular structure of the produced films, irrespectively of the film side of analysis (upper and down).

Regarding the thermal features of the casted films obtained from DSC, the observed transitions match those previously reported in literature (Kamide and Saito 1985; Kennedy et al. 1995; Zugenmaier 2004). Melting temperatures in the range 226°C-233°C (Fig. 6.) where observed, which is in accordance with the wide range of melting temperatures reported for cellulose acetate (from 220°C – 300°C), depending on the degree of acetylation (Barud et al. 2008; Yadollahi et al. 2019). However, glass transition was not detected in all casted films in first heating scan. Similar “absence” of T_g is already reported for some commercial samples (Zugenmaier 2004; Kamide 2005). The “absence” of glass transition temperature may be explained as it is actually a baseline shift toward endothermic range rather than obvious transition (Kamide 2005). With the first heating scan in this investigation, glass transition temperature, T_g, was only clearly observed in the case of the CA film prepared on glass at open air, at 195 ± 2°C, a value similar to previously reported data for cellulose acetate (Zugenmaier 2004).

Melting temperatures and enthalpies of fusion were determined from the first heating scan. The degree of crystallinity was calculated for all films casted under different conditions from 10% CA solution in

acetone (Fig. 6).

Casting under different conditions led to changes in melting enthalpy and crystallinity. As can be seen, the material with the lowest crystallinity (casted on glass at open air) is the one for which the T_g was detectable. Therefore, it could be that degree of crystallinity is the main cause of observation of T_g. High crystallinity degree may make the detection of T_g difficult because of low DSC sensitivity and possible overlapping of the endotherm glass transition and melting signals.

On the other hand, for CA films under this study the crystallinity degree could be related to evaporation rate of the solvent during drying of films. When films are casted on open air, uncontrolled airflow above solution causes faster evaporation and molecules have less time to organize, therefore, crystallinity is the lowest in films casted on open air. On the contrary, when films are casted in a closed environment, there is a less disturbance from the airflow, causing slower evaporation of acetone, giving enough time to macromolecules to organize. Additionally, by comparing films casted in open air on different surfaces we can conclude that much higher order is present in cellulose acetate casted on PTFE surface, compared to the materials casted on glass, which had the lowest melting enthalpy of all analyzed samples, even lower than initial powder cellulose acetate. This result is in accordance with the results obtained by Liu and Hsieh (Liu and Hsieh 2002) where lower value of enthalpy of fusion was measured using DSC for casted cellulose acetate film compared to powder cellulose acetate.

As it was said in previous section, the whitish appearance of films casted on glass at 75% humidity was tentatively explained considering that increase of humidity yields increase of crystallinity causing reduction of transparency because of light scattering. The same reason could be used to explain translucent behavior of PTFE casted film. However, results from DSC are not completely in accordance with this explanation of the optical behaviors. For example, crystallinity is higher for translucent PTFE casted films on open air compared to the transparent films casted on glass in open air. However, the films casted under controlled humidity have similar crystallinity to PTFE casted films on open air and they are completely transparent. Once again, the results point out as an only explanation of the different optical behavior the surface patterns generated in the film depending on the substrate surface used to carry out the casting process.

In the particular case of the slight transparency decrease found for the film prepared under the humidity of 75%, it can be explained considering phase separation process. Evaporation, when humidity is high enough, may lead to a phase separation process since water is a precipitant for cellulose acetate dissolved in acetone. Therefore, it could be expected certain phase separation on the upper side of the films (the one directly in contact with moisture) as if cellulose acetate powder was being formed. In fact, films obtained under 75% of humidity had similar values of crystallinity as powder of CA. In order to corroborate this, 10% CA solution in acetone was casted under 90% humidity, which resulted in white spots all over the surface of the film (Fig. 7).

Therefore, in terms of transparency, having in mind the results obtained from morphology and crystallinity, the most optimal conditions for film casting should be 55% humidity in a closed chamber using glass modified dishes, looking for three different effects: i) to slow down the evaporation rate; ii) to reduce the possibility of turbulent air flow during drying; and iii) to reduce the heterogeneity of the substrate surface, which can affect morphology, optical appearance and thermal properties of films.

Regarding the films casted on PTFE, their translucency is not related to crystallinity either, rather than to the morphology of film. As it was seen in the optical images, the patterned surface of film, more precisely the side of the film that was close to the dish, adopted the pattern from PTFE dish, and this pattern causes scattering of light similar to the so called etched glass.

Namely, etched glass is made when surface of glass is altered by etching, creating nano and microroughness which can cause transmitted light to scatter and may cause various optical effects (Fouckhardt et al. 2007). High surface roughness according to other researches, enhances surface hydrophobicity, and additionally transforms the transparent glass to translucent or opaque due to light scattering (Chen et al. 2018; Liu et al. 2021).

3.3. Wettability of casted films and optical tunability upon wetting of patterned films casted on PTFE

Cellulose acetate is generally less hydrophilic than cellulose, due to the substituted OH groups by acetyl ones. However, acetate films are not totally hydrophobic and their contact angle is usually lower than 90°, as reported for solution casted (Wu et al. 2014) or spin-coated thin CA films (Mikaeili and Gouma 2018) .

The static contact angle using the sessile drop method was measured on both sides of each film (Fig. 8. and Fig. 9), for films casted on glass and on PTFE, respectively. There was no clear correlation between humidity during casting of films and wettability (Fig. 8.), but clear influence of patterned surface of PTFE film on wettability (Fig. 9.) can be noticed.

The wettability tests, i.e. measurements of static contact angle, were performed up to 5 min upon contact of water and surface. In all samples, there was a little decrease of contact angle over time (up to 10% of the starting contact angle value, in the first 5 min after the contact of the surface with water). Therefore, before 1 minute no change of water contact angle is expected.

In general, the highest contact angle was measured in films casted on PTFE surface in open air, without humidity control. Higher wettability (lower water contact angle) was measured in samples casted on PTFE at 55% humidity compared to the same one casted in open air (Fig. 9). As expected, the lowest wettability was detected on patterned surfaces, i.e. surfaces of films which were in contact with the patterned PTFE dish (Fig. 9).When observing water contact angles on both sides of films casted on glass, the differences are within the measurement error compared to films casted under controlled humidity. However, when there is not humidity control (open air) significant differences appear depending on the

upper and down sides. As can be seen from Fig. 9, for films casted on PTFE dish, contact angle of patterned down side is 32% higher than contact angle of upper side of film.

Moreover, an interesting effect was noticed in samples casted on PTFE. The patterned side, when wetted, becomes transparent, a result that was also confirmed using optical microscopy (Fig. 10). Upon wetting, the surface of films is more even due to the fact that water (with similar diffraction index as film) fills channels on the surface, rendering the film transparent. This optical effect is completely reversible: water can be removed from the surface by simple wiping and translucency is recovered.

Thus, the films prepared in this work, specifically those obtained on PTFE surface, can have potential applications in food packaging, as they become transparent and change transparency when wetted, which could be useful as an indicator for increased moisture within the food package. Hence, it can be proposed to use tunable translucent side as the inner side of packaging, while the opposite side could be used as the outer side. The micropatterning that occurs during casting of films from the use of controlled topography of the substrate can be further explored for obtaining other different optical effects. Tunable optical effects induced by micropatterning can be used to design sensors in active food packaging application, avoiding for instance addition of chemical and biological additives (Mustafa and Andreescu 2018).

Conclusions

In this work, preparation of cellulose acetate films using solution casting method was performed using different surfaces (borosilicate glass, soda-lime glass and PTFE) and under different humidity conditions. It was found that casting under controlled humidity increases the crystallinity of films, obtaining a highest value of crystallinity when casting at 55% humidity on soda-lime glass surface coated with chlorotrimethylsilane. Additionally, visual appearance of films in terms of smoothness of the surface and high transparency was achieved when 55% humidity was maintained during drying of films. ATR-FTIR did not reveal any changes in the molecular structure of the films induced by casting conditions, but the DSC analyses showed that melting temperature increases with increasing humidity during casting, exhibiting the highest values when films were casted at 75% humidity. Cellulose acetate films casted on patterned PTFE surface exhibited optical anisotropy because the CA side directly in contact with the PTFE adopted its pattern. Resulting films were translucent, but when patterned side was wetted, they became transparent. This result can be used for producing packaging films with tunable transparency in a straightforward manner, changing their morphology with an adequate section of a patterned casting surface.

Declarations

Funding

This work was financially supported by CONEX-Plus program of Universidad Carlos III de Madrid (UC3M) and the European Commission through the Marie-Sklodowska Curie COFUND Action (Grant Agreement No 801538). Authors also appreciate the financial support received from AEI (Ministerio de Ciencia e Innovación of Spain, PID2020-112713RB-C22 and –C21]; the Universidad Carlos III de Madrid, Fondos de Investigación of Fco. Javier González Benito [2012/00130/004] and the strategic Action in Multifunctional Nanocomposite Materials [Code: 2011/00287/003].

Conflict of interest/competing interest

The authors have no relevant financial or non-financial interests to disclose

Availability of data and material

Not applicable.

Code availability

Not applicable.

Authors' contributions

Conceptualization [Ana Kramar, Javier González-Benito]; Methodology, Investigation, Formal analysis, Validation [Ana Kramar, Irene Rodríguez Ortega, Gustavo González-Gaitano, Javier González-Benito]; Writing-original draft [Ana Kramar]; Writing - Review & Editing [Irene Rodríguez Ortega, Gustavo González-Gaitano, Javier González-Benito]; Supervision [Javier González-Benito]

Ethical approval and ethical standards

Not applicable.

Acknowledgement

This work was financially supported by CONEX-Plus program of Universidad Carlos III de Madrid (UC3M) and the European Commission through the Marie-Sklodowska Curie COFUND Action (Grant Agreement No 801538). Authors also appreciate the financial support received from AEI (Ministerio de Ciencia e Innovación of Spain, PID2020-112713RB-C22 and –C21]; the Universidad Carlos III de Madrid, Fondos de Investigación of Fco. Javier González Benito [2012/00130/004] and the strategic Action in Multifunctional Nanocomposite Materials [Code: 2011/00287/003].

References

1. Barud HS, Ara AM, De, Santos DB et al (2008) Thermal behavior of cellulose acetate produced from homogeneous acetylation of bacterial cellulose. 471:61–69. https://doi.org/10.1016/j.tca.2008.02.009

2. Cerqueira DA, Filho GR, Assunção RMN (2006) A New Value for the Heat of Fusion of a Perfect Crystal of Cellulose Acetate. 484:475–484. https://doi.org/10.1007/s00289-006-0511-9
3. Chen Z, Li G, Wang L et al (2018) A strategy for constructing superhydrophobic multilayer coatings with self-cleaning properties and mechanical durability based on the anchoring effect of organopolysilazane. Mater Des 141:37–47. https://doi.org/10.1016/j.matdes.2017.12.034
4. De Carvalho Eufrásio Pinto M, Da Silva D, Amorim Gomes D et al (2019) Film based on magnesium impregnated biochar/cellulose acetate for phosphorus adsorption from aqueous solution. RSC Adv 9:5620–5627. https://doi.org/10.1039/c8ra06655h
5. Do Socorro Rocha Bastos M, Da Silva Laurentino L, Canuto KM et al (2016) Physical and mechanical testing of essential oil-embedded cellulose ester films. Polym Test 49:156–161. https://doi.org/10.1016/j.polymertesting.2015.11.006
6. El Fawal GF, Omer AM, Tamer TM (2019) Evaluation of antimicrobial and antioxidant activities for cellulose acetate films incorporated with Rosemary and Aloe Vera essential oils. J Food Sci Technol 56:1510–1518. https://doi.org/10.1007/s13197-019-03642-8
7. Espitia PJP, Soares NDFF, Botti LCM, Silva WA (2011) Effect of essential oils in the properties of cellulosic active packaging. Macromol Symp 299–300:199–205. https://doi.org/10.1002/masy.200900124
8. Figueiredo AS, Garcia AR, Minhalma M et al (2020) The ultrafiltration performance of cellulose acetate asymmetric membranes: A new perspective on the correlation with the infrared spectra. J Membr Sci Res 6:70–80. https://doi.org/10.22079/JMSR.2019.110424.1269
9. Filho GR, Chagas R, Meireles S et al (2004) Water Flux through Blends from Waste Materials: Cellulose Acetate (from Sugar Cane Bagasse) with Polystyrene (from Plastic Cups). https://doi.org/10.1002/app.21474
10. Fouckhardt H, Steingoetter I, Brinkmann M et al (2007) Nm- and µm-scale surface roughness on glass with specific optical scattering characteristics on demand. Adv Optoelectron 2007:. https://doi.org/10.1155/2007/27316
11. Gonçalves SM, dos Santos DC, Motta JFG et al (2019) Structure and functional properties of cellulose acetate films incorporated with glycerol. Carbohydr Polym 209:190–197. https://doi.org/10.1016/j.carbpol.2019.01.031
12. Gopi S, Pius A, Kargl R et al (2019) Fabrication of cellulose acetate/chitosan blend films as efficient adsorbent for anionic water pollutants. Polym Bull 76:1557–1571. https://doi.org/10.1007/s00289-018-2467-y
13. Harini K, Sukumar M (2019) Development of cellulose-based migratory and nonmigratory active packaging films. Carbohydr Polym 204:202–213. https://doi.org/10.1016/j.carbpol.2018.10.018
14. Kamide K (ed) (2005) Cellulose and cellulose derivatives Molecular characterization and its applications. Elsevier
15. Kamide K, Saito M (1985) Thermal Analysis of Cellulose Acetate Solids with total Degrees of Substitution of 0.49, 1.75, 2.46, and 2.92. Polym J 17:919–928

16. Kennedy JF, Phillips GO, Williams PA, Piculell L (eds) (1995) Cellucon '93 proceedings Cellulose and cellulose derivatives: Physico-chemical aspects and industrial applications. Woodhead Publishing Limited
17. Liu H, Hsieh Y, Lo (2002) Ultrafine fibrous cellulose membranes from electrospinning of cellulose acetate. J Polym Sci Part B Polym Phys 40:2119–2129. https://doi.org/10.1002/polb.10261
18. Liu P, Bai X, Xing W et al (2021) Translucent and superhydrophobic glass for self-cleaning and acid rain-restraining. Mater Chem Phys 259:124049. https://doi.org/10.1016/j.matchemphys.2020.124049
19. Lyytikäinen J, Morits M, Österberg M et al (2021) Skin and bubble formation in films made of methyl nanocellulose, hydrophobically modified ethyl(hydroxyethyl)cellulose and microfibrillated cellulose. Cellulose 28:787–797. https://doi.org/10.1007/s10570-020-03557-0
20. Menachem L (ed) (2007) Handbook of fiber chemistry. CRC Press Taylor& Francis Group
21. Mikaeili F, Gouma PI (2018) Super Water-Repellent Cellulose Acetate Mats. Sci Rep 8:1–8. https://doi.org/10.1038/s41598-018-30693-2
22. Mirvakili MN, Hatzikiriakos SG, Englezos P (2021) Opaque and translucent films from aqueous microfiber suspensions by evaporative self-assembly. Phys Fluids 33. https://doi.org/10.1063/5.0043881
23. Mustafa F, Andreescu S (2018) Chemical and biological sensors for food-quality monitoring and smart packaging. Foods 7. https://doi.org/10.3390/foods7100168
24. Paunonen S (2013) Strength and barrier enhancements of cellophane and cellulose derivative films: A review. BioResources 8:3098–3121. https://doi.org/10.15376/biores.8.2.3098-3121
25. Rodríguez FJ, Abarca RL, Bruna JE et al (2019) Effect of organoclay and preparation method on properties of antimicrobial cellulose acetate films. Polym Compos 40:2311–2319. https://doi.org/10.1002/pc.25041
26. Shivamurthy B, Thimmappa BHS, Purushothama R, Datta Sai GKVD (2019) Electrical Conductivity and Mechanical Properties of Dendritic Copper Particulate Polymer Films. Trans Electr Electron Mater 20:99–106. https://doi.org/10.1007/s42341-018-00085-4
27. Vartiainen J, Vähä-Nissi M, Harlin A (2014) Biopolymer Films and Coatings in Packaging Applications—A Review of Recent Developments. Mater Sci Appl 05:708–718. https://doi.org/10.4236/msa.2014.510072
28. Vinodhini PA, Sangeetha K, Thandapani G et al (2017) FTIR, XRD and DSC studies of nanochitosan, cellulose acetate and polyethylene glycol blend ultrafiltration membranes. Int J Biol Macromol 104:1721–1729. https://doi.org/10.1016/j.ijbiomac.2017.03.122
29. Wu S, Qin X, Li M (2014) The structure and properties of cellulose acetate materials: A comparative study on electrospun membranes and casted films. J Ind Text 44:85–98. https://doi.org/10.1177/1528083713477443
30. Xie J, Hung YC (2019) Methodology to evaluate the antimicrobial effectiveness of UV-activated TiO2 nanoparticle-embedded cellulose acetate film. Food Control.

https://doi.org/10.1016/j.foodcont.2019.06.016. 106:

31. Yadollahi R, Dehghani Firouzabadi M, Mahdavi H et al (2019) How properties of cellulose acetate films are affected by conditions of iodine-catalyzed acetylation and type of pulp. Cellulose 26:6119–6132. https://doi.org/10.1007/s10570-019-02510-0
32. Yang ZY, Wang WJ, Shao ZQ et al (2013) The transparency and mechanical properties of cellulose acetate nanocomposites using cellulose nanowhiskers as fillers. Cellulose 20:159–168. https://doi.org/10.1007/s10570-012-9796-z
33. Zugenmaier P (2004) Characteristics of cellulose acetate. 81–166. https://doi.org/10.1002/masy.200450407
34. European committee for standardization (1997) Surface texture: Profile method-Rules and procedures for the assessment of surface texture (ISO 4288: 1997)

Figures

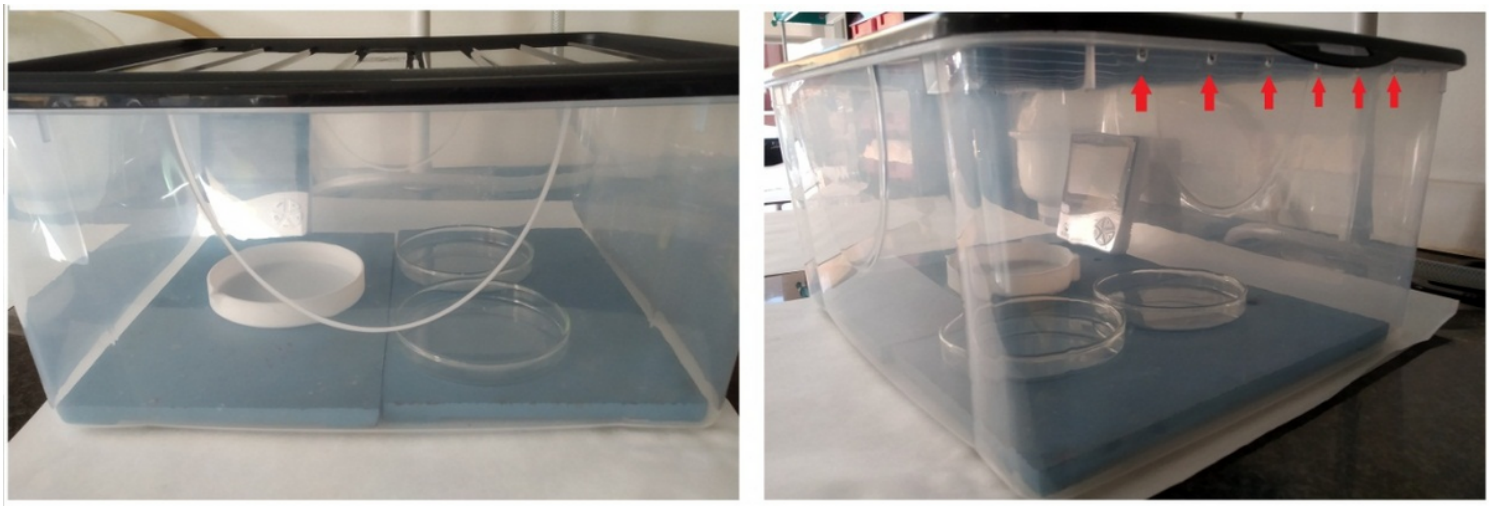

Figure 1

Perforated box (red arrows) used to keep constant the relative humidity during the casting of CA films.

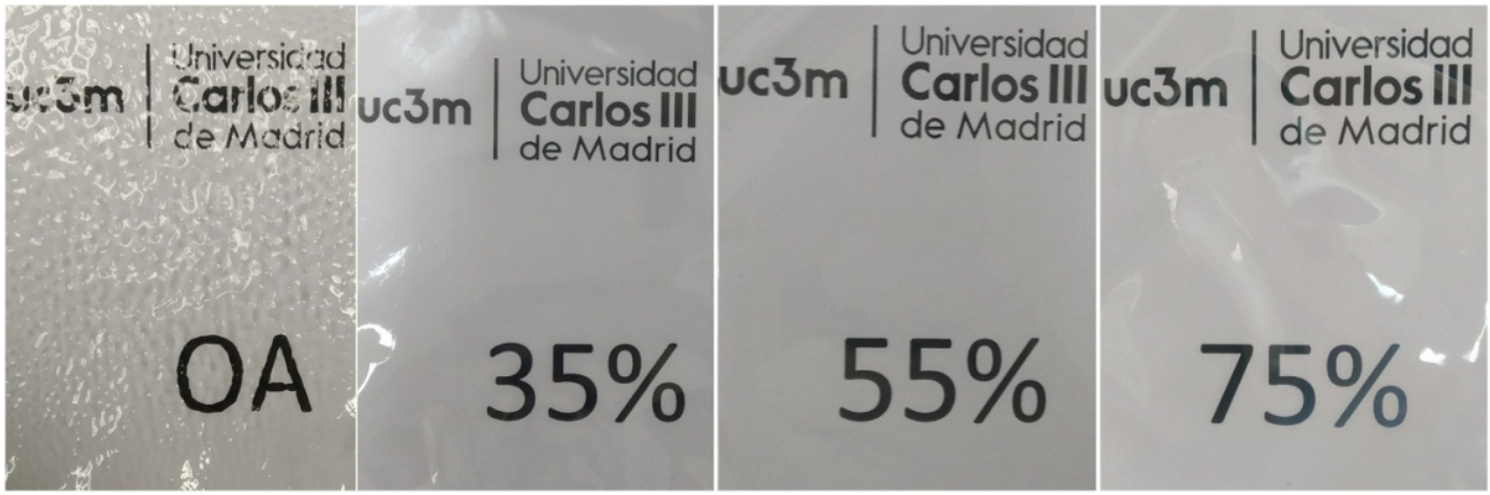

Figure 2

Visual appearance of cellulose acetate films prepared by solution casting method at open air (OA) and at different humidity (35 %, 55 % and 75 %).

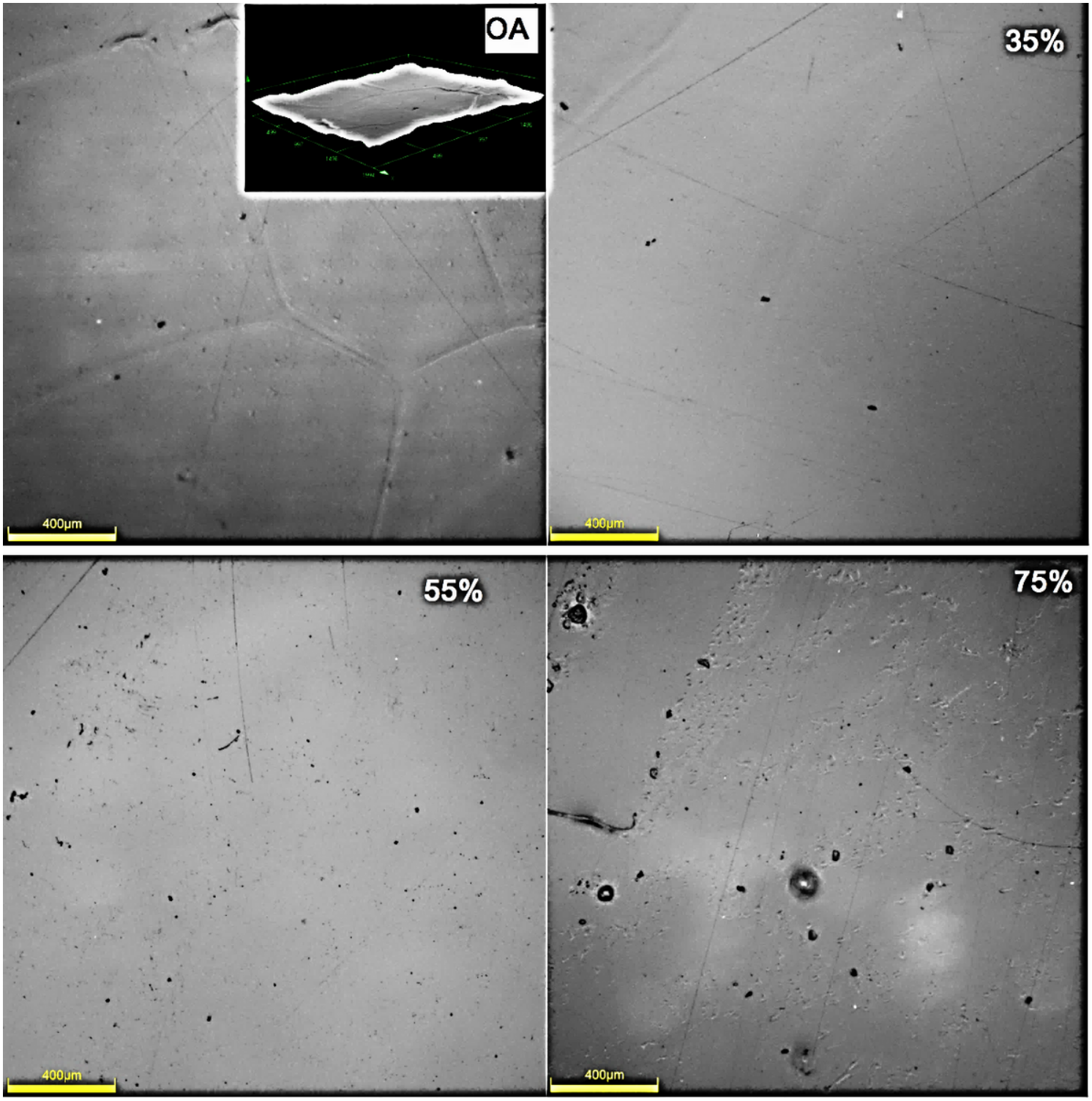

Figure 3

Cellulose acetate film casted on a glass surface from a 8% acetone solution at open air (OA) and at different humidity conditions (35 %, 55 %, 75 %).

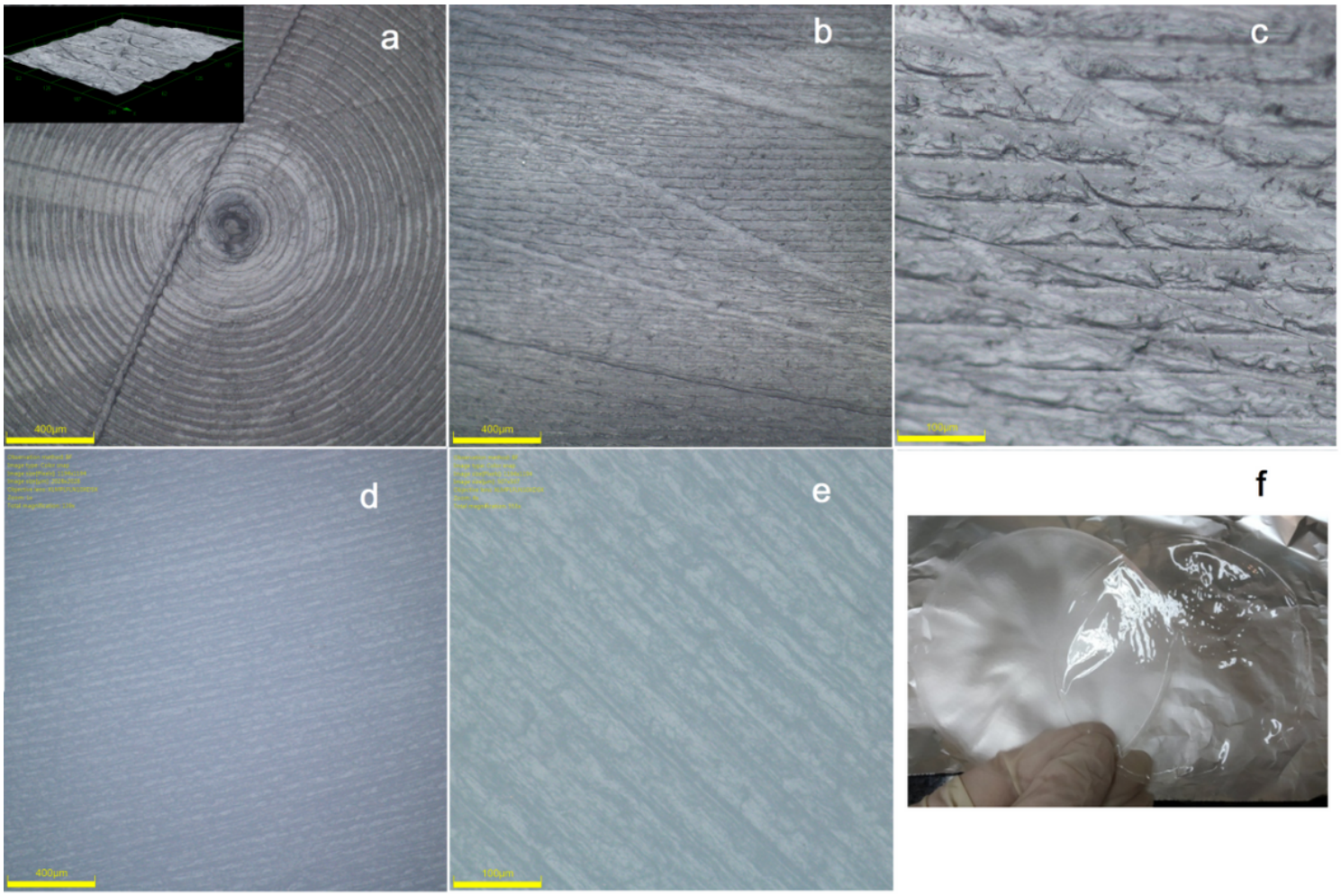

Figure 4

Cellulose acetate film casted from a 12 % solution in acetone on a patterned PTFE dish. a) Center of the film surface in contact with the dish during drying; inset of a 3D image at higher magnification; b) film surface far from the center of the casted film; c) higher magnification of the region of observation represented by the image b; d) surface of PTFE dish at the same magnification as in b; e) surface of PTFE dish at the same same magnification as c and f) visual aspect of films casted on PTFE surface (translucent) and flat glass (transparent), respectively.

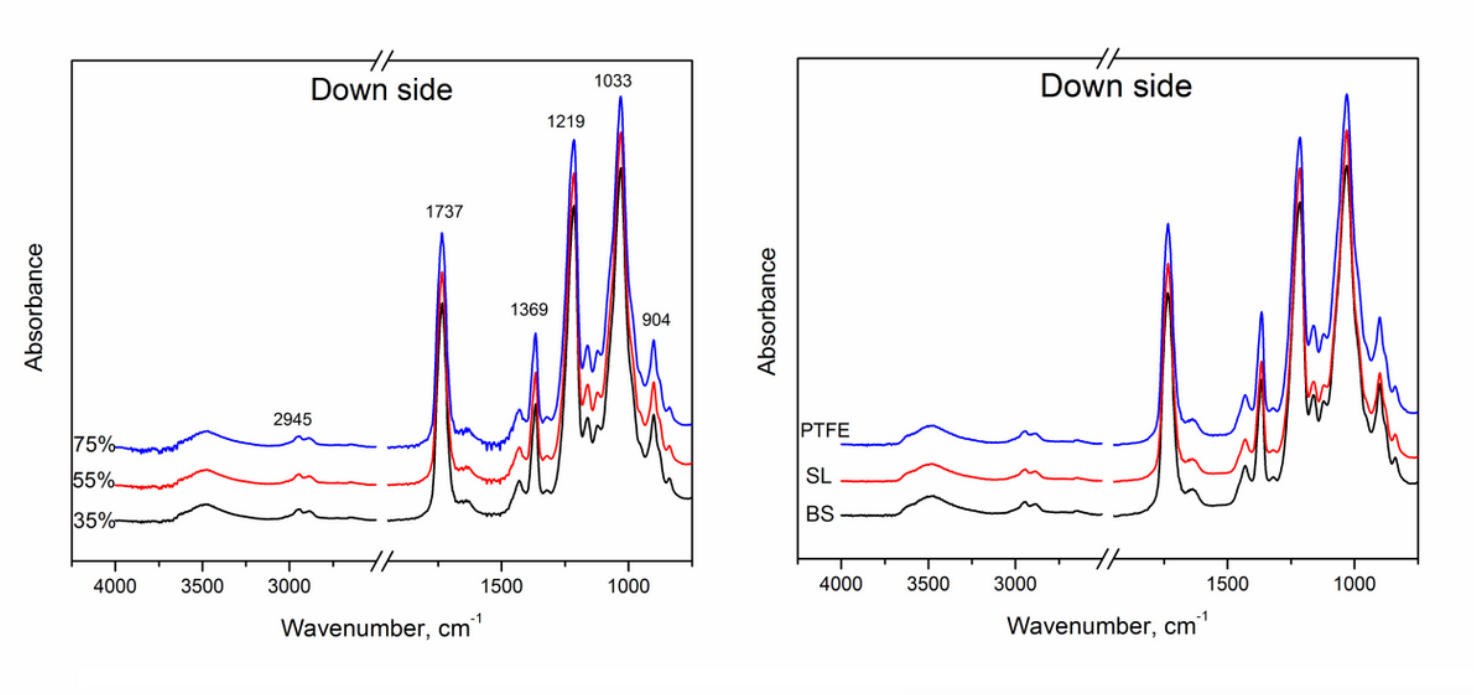

Figure 5

ATR-FTIR spectra of casted cellulose acetate films (down side) under various humidity conditions (35 %, 55 %, 75%) and on different surfaces (PTFE-teflon, SL- soda lime glass coated with chlorotrimethylsilane, BS-borosilicate glass)

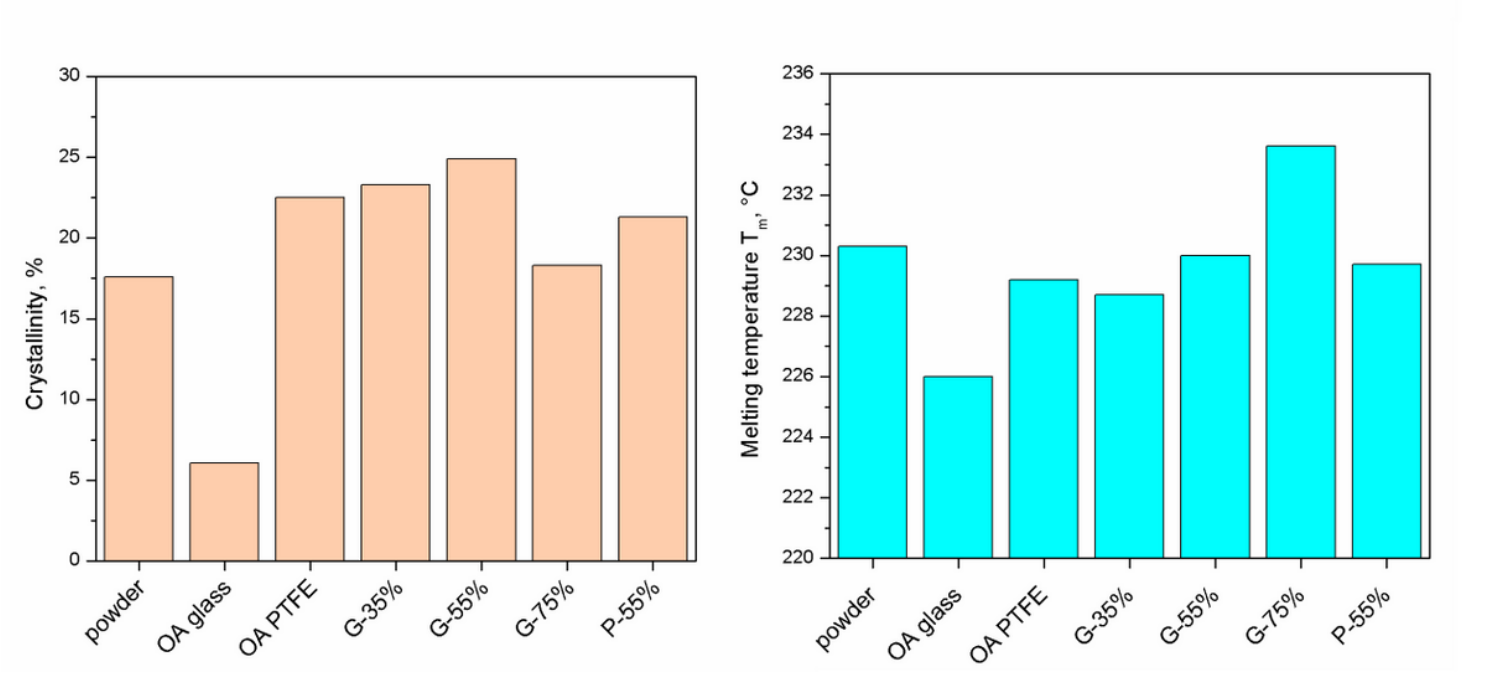

Figure 6

Crystallinity and peak melting temperatures of various cellulose acetate films prepared from 10 % concentration of CA in acetone under various humidity and in open air (OA)

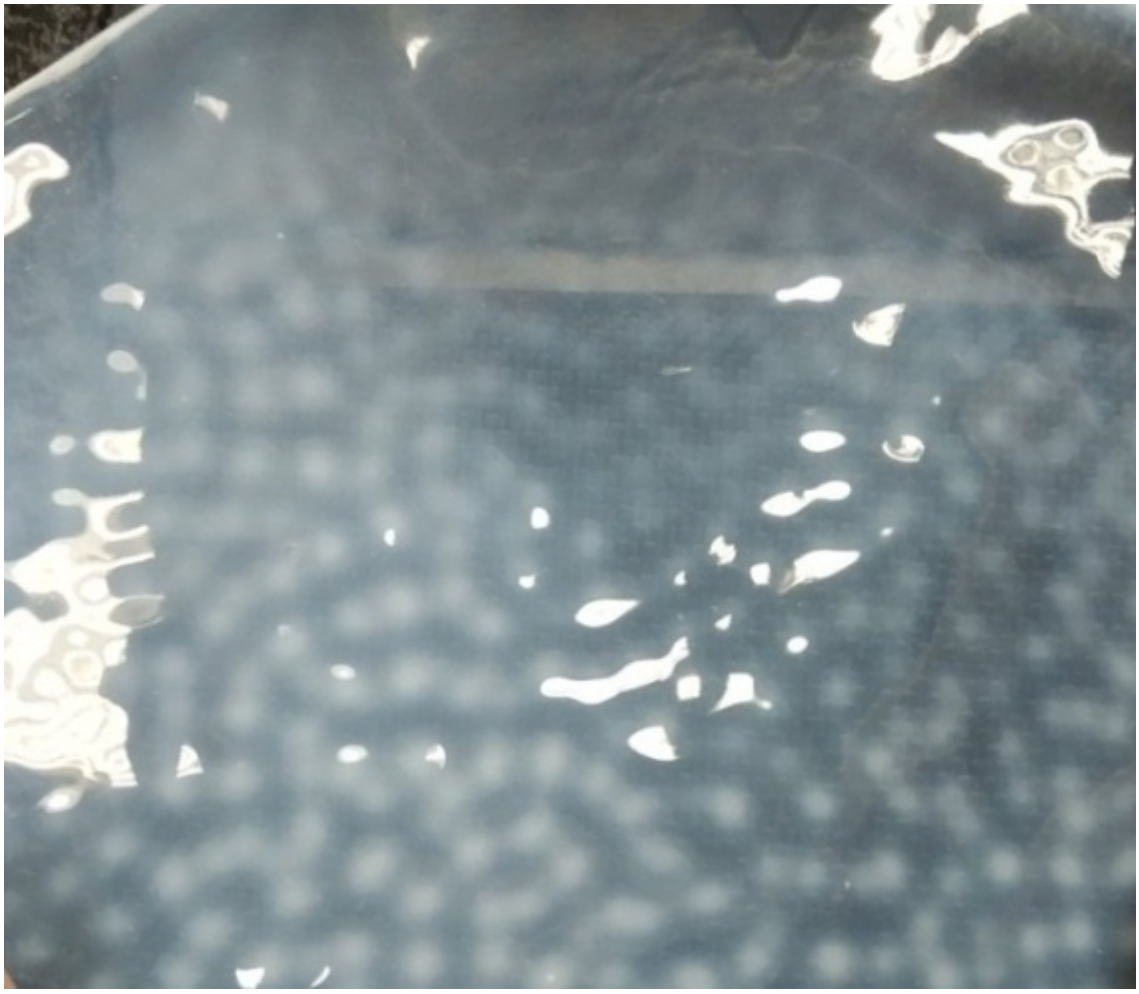

Figure 7

Appearance of cellulose acetate film casted at 90 % humidity.

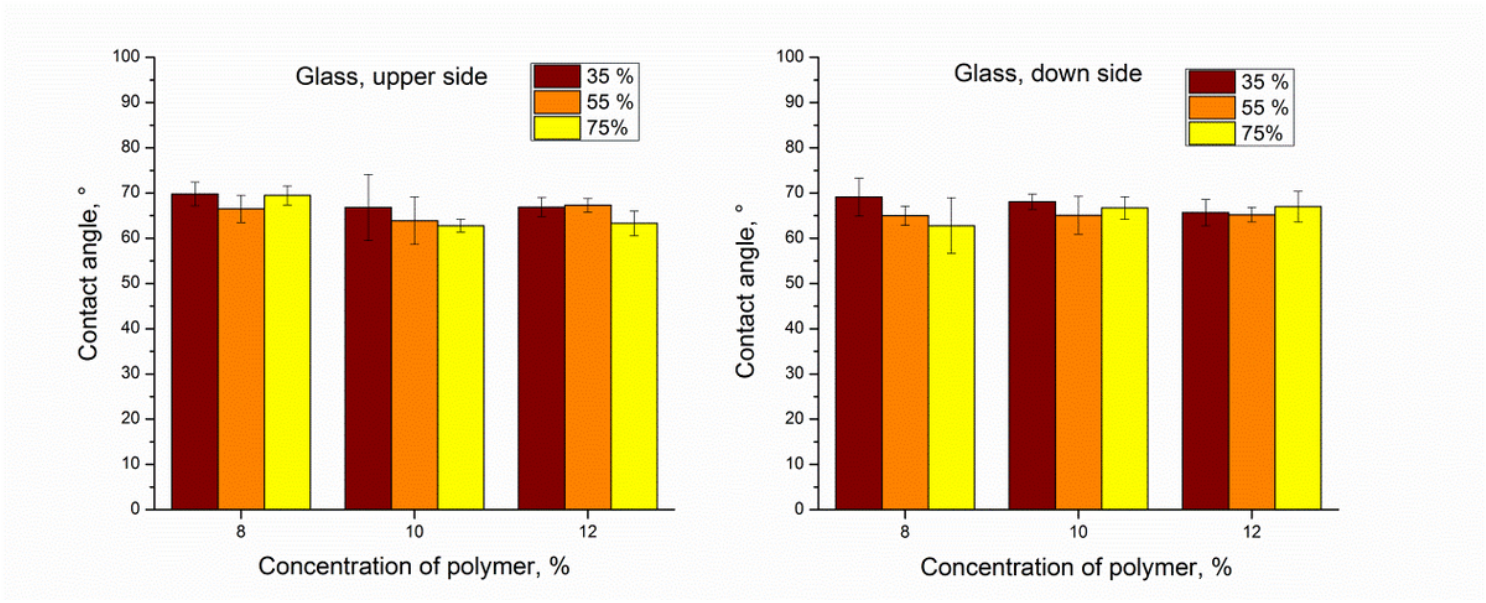

Figure 8

Contact angle values on upper and down sides of films casted on soda-lime coated glass at 35 %, 55 % and 75 % humidity.

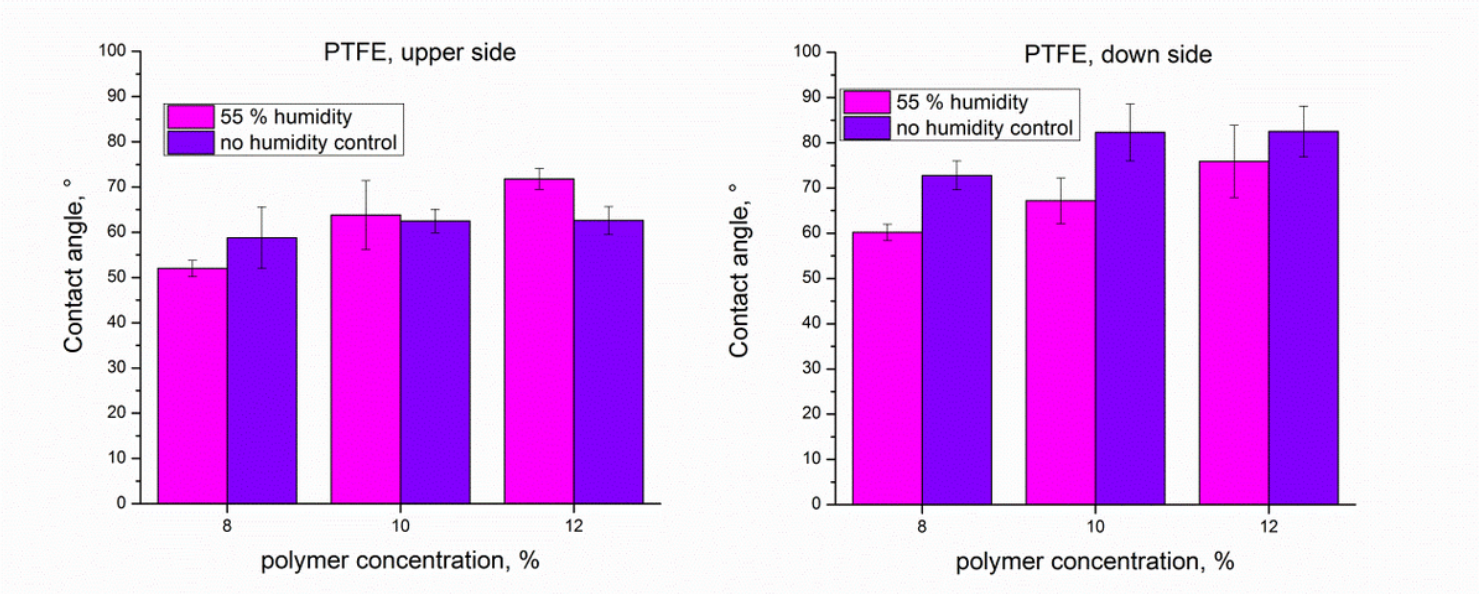

Figure 9

Contact angle values of upper and down sides of films casted on PTFE surface at controlled humidity (55 %) and on open air (no humidity and air flow control).

Figure 10

Macroscopic (top) appearance of cellulose acetate patterned films obtained on PTFE surface, in dry (left) and wet (right) state and microphotograph of corresponding surfaces (bottom); circular translucent film

with wetted central part showing difference in transparency